HHS Public Access

Author manuscript

Glycoconj J. Author manuscript; available in PMC 2020 October 13.

Published in final edited form as:

Glycoconj J. 2019 April ; 36(2): 165–174. doi:10.1007/s10719-019-09863-5.

Glycosaminoglycans compositional analysis of Urodele axolotl (*Ambystoma mexicanum*) and Porcine Retina

So Young Kim[1], **Joydip Kundu**[2], **Asher Williams**[3], **Anastasia S. Yandulskaya**[4], **James R. Monaghan**[4], **Rebecca L. Carrier**[2], **Robert J. Linhardt**[1,3,5,6,7]

[1]Biochemistry and Biophysics Graduate Program, Center for Biotechnology and Interdisciplinary Studies, Rensselaer Polytechnic Institute, Troy, NY 12180, USA

[2]Department of Chemical Engineering, Northeastern University, Boston, MA 02115, USA

[3]Department of Chemical and Biological Engineering, Center for Biotechnology and Interdisciplinary Studies, Rensselaer Polytechnic Institute, Troy, NY, USA

[4]Department of Biology, Northeastern University, Boston, MA, USA

[5]Department of Biological Science, Center for Biotechnology and Interdisciplinary Studies, Rensselaer Polytechnic Institute, Troy, NY, USA

[6]Department of Chemistry and Chemical Biology, Center for Biotechnology and Interdisciplinary Studies, Rensselaer Polytechnic Institute, Troy, NY, USA

[7]Department of Biomedical Engineering, Center for Biotechnology and Interdisciplinary Studies, Rensselaer Polytechnic Institute, Troy, NY, USA

Abstract

Retinal degenerative diseases, such as age-related macular degeneration (AMD) and retinitis pigmentosa (RP), are major causes of blindness worldwide. Humans cannot regenerate retina, however, axolotl (*Ambystoma mexicanum*), a laboratory-bred salamander, can regenerate retinal tissue throughout adulthood. Classic signaling pathways, including fibroblast growth factor (FGF), are involved in axolotl regeneration. Glycosaminoglycan (GAG) interaction with FGF is required for signal transduction in this pathway. GAGs are anionic polysaccharides in extracellular matrix (ECM) that have been implicated in limb and lens regeneration of amphibians, however, GAGs have not been investigated in the context of retinal regeneration. GAG composition is characterized native and decellularized axolotl and porcine retina using liquid chromatography mass spectrometry. Pig was used as a mammalian vertebrate model without the ability to regenerate retina. Chondroitin sulfate (CS) was the main retinal GAG, followed by heparan sulfate (HS), hyaluronic acid, and keratan sulfate in both native and decellularized axolotl and porcine retina. Axolotl retina exhibited a distinctive GAG composition pattern in comparison with porcine retina, including a higher content of hyaluronic acid. In CS, higher levels of 4- and 6-*O*-sulfation were observed in axolotl retina. The HS composition was greater in decellularized tissues in both

✉Rebecca L. Carrier rebecca@coe.neu.edu; Robert J. Linhardt linhar@rpi.edu.

Conflicts of interest The authors declare to haveno conflicts of interest.

Ethical approval Animals in this study were approved by Institutional Animal Care and Use Committee (IACUC).

axolotl and porcine retinaby 7.1% and 15.4%, respectively, and different sulfation patterns were detected in axolotl. Our findings suggest a distinctive GAG composition profile of the axolotl retina set foundation for role of GAGs in homeostatic and regenerative conditions of the axolotl retina and may further our understanding of retinal regenerative models.

Keywords

Amphibian; Axolotl; Glycosaminoglycans; Regeneration; Retina

Introduction

Globally, hundreds of millions of people are projected to suffer from varying levels of vision loss caused by retinal degenerative diseases by 2020, with age-related macular degeneration (AMD) and retinitis pigmentosa (RP) being the most prevalent forms of these diseases [1]. Currently, there are no treatment options available for RP and while several treatments are available for AMD, including anti-angiogenesis and laser therapy, these are costly and are not accessible to all patients in parts of the world. While humans do not possess retinal regenerative capability, many animals do at various developmental stages. However, some vertebrates, including amphibians and fish, maintain this ability for retinal regeneration at maturity. Retinal regeneration can rely on a number of factors including: 1) activation of neural retina-supportive cells from Muller glia cells/retinal pigmented epithelium (RPE); 2) activation of stem/progenitor cells residing in ciliary body (CB)/ciliary marginal zone (CMZ) to ultimately differentiate into retinal cells; and 3) contributing extracellular matrix (ECM) components, particularly during regeneration [2–4]. All classic cell signaling pathways involved, including wingless (Wnt), bone morphogenetic protein (BMP), and fibroblast growth factor/mitogen-activated protein kinase (FGF/MAPK), are conserved between salamanders and mammals. In particular, the FGF/MAPK pathway activation leads to regulation of the common downstream effector paired box protein (Pax6) [5–8].

The FGF signaling pathway requires binding to fibroblast growth factor receptor (FGFR) with a glycosaminoglycan (GAG) in a 2:2:2 complex for cellular signal transduction [9, 10]. GAGs are anionic linear polysaccharides comprised of repeating disaccharide units and are found on the external surface of cell membranes and as major components of the ECM. GAGs have important biological functions including in cellular communication; cell migration, proliferation, and adhesion; pathogenesis; immunity; and wound healing [11–13]. There are four main types of GAGs: hyaluronan (HA), heparan sulfate (HS), chondroitin sulfate (CS), and keratan sulfate (KS), that vary in disaccharide sequence, sulfation pattern, and molecular weights. Except HA, all GAGs are covalently attached to various core proteins, making up proteoglycans (PGs). GAGs are implicated in various types of retinal degenerative diseases, including rhegmatogenous retinal detachment (RRD), AMD, and mucopolysaccharidosis (MPS) type-I associated retinal degeneration [14–22]. A decreased level of HA and higher hyaluronidase catalytic activity has been found in RRD patients [14]. HS plays a critical role in choroidal neovascularization (CNV) and complement activation system of AMD. HS regulates CNV by interacting with various angiogenic growth factors including FGF, upregulates HS-PG expression in CNV lesions, and is linked to the

endothelial dysfunction and increased capillary permeability [15–19]. In AMD, specific genetic variants of complement factor H (CFH), a key regulator in complement system's alternative pathway, can lose their ability to properly bind to HS, leading to inactivation of CFH [15–22].

The role of GAGs in regeneration of limbs and eyes has also been described in anurans, fish, ophiuroids, and urodeles. Upregulated HA synthesis allows successful limb-tail regeneration without scarring by providing a highly hygroscopic and immunosuppressed ECM environment in amphibians and lizards [23]. Similarly, HA synthesis is required in tail fin regeneration of zebrafish [24]. In lens regeneration of urodele newts, the accumulation of HA has been implicated in the de-differentiation of iris epithelial cells and upregulation of hyaluronidase in accelerating turnover and remodeling of ECM required for cell-type conversion [25]. HS greatly contributes to the ability of cells to remember the original specific position of ECM when recreating missing patterns during limb development in mouse, rat, chick, anuran *Xenopus,* and urodele axolotl, as well as limb regeneration in the latter two species [26, 27]. Similarly, the expression of enzymes involved in CS biosynthesis is upregulated and the specific sulfation pattern is required for successful arm regeneration in ophiuroids *Amphiura filiformis* (brittle star) [28]. In teleost zebrafish, however, CS showed repelling behavior in retinal axonal regeneration [29]. There are extensive reports of the ability of CS to both inhibit and enhance regeneration of neural tissues [30, 31].

Among the best available vertebrate models of regeneration are urodele axolotls and newts, as they are the only known tetrapods with regenerative ability of complex body parts including limb, central nervous system (CNS) and portions of their eyes throughout their entire lifespan [32, 33]. Urodeles can perform reparative neurogenesis during adulthood in different regions of the CNS, including the forebrain, midbrain, spinal cord, and retina [34]. The genome of axolotl *(Ambystoma mexicanum)* has recently been decoded as 32 gigabase-pairs, which is 14 times larger than the anuran Xenopus genome and 10 times larger than the human genome [35, 36]. *The urodele axolotl is the most often bred salamander species in the laboratory and* is a well-developed model for embryology, retinal neuron processing and regeneration [37, 38]. While the importance of the specific role of GAGs in signaling in axolotl limb regeneration is established and there are extensive reports on the role of retinal GAGs across species, the structure and role of GAGs in retina tissue of axolotl has not yet been investigated. Here, we describe the use of disaccharide compositional analysis by liquid chromatography mass spectrometry (LCMS) to characterize structure of GAGs from axolotl retina as a retinal regenerative model, and compare these to porcine retinal GAGs as a mammalian retina without regenerative capability. We have also analyzed decellularized axolotl and porcine retina to investigate the difference in GAG content between retina tissue and ECM. To our knowledge, this is the first characterization of retinal GAG isolated from urodele axolotl, laying the groundwork for further investigation of the biological functions of GAGs in the axolotl retina during homeostasis and regeneration.

Materials and methods

Materials

Unsaturated disaccharide standards of CS (ΔUA-GalNAc; ΔUA-GalNAc4S; ΔUA-GalNAc6S; ΔUA2S-GalNAc; ΔUA2S-Gal-NAc4S; ΔUA2S-GalNAc6S; ΔUA-GalNAc4S6S; ΔUA2S-GalNAc4S6S), unsaturated disaccharide standards of HS (ΔUA-GlcNAc; ΔUA-GlcNS; ΔUA-GlcNAc6S; ΔUA2S-GlcNAc; ΔUA2S-GlcNS; ΔUA-GlcNS6S; ΔUA2S-GlcNAc6S; ΔUA2S-GlcNS6S), and unsaturated disaccharide standard of HA (ΔUA-GlcNAc), where ΔUA is 4-deoxy-α-L-*threo*-hex-4-enopyranosyluronic acid, S is sulfo and Ac is acetyl, were from Iduron (UK). Actinase E was obtained from Kaken Biochemicals (Tokyo, Japan). Chondroitin lyase ABC from *Proteus vulgaris* was expressed in *Escherichia coli* in our laboratory. Recombinant *Flavobacterial* heparinase I, II, and III were expressed in our laboratory using *E. coli* strains that were gifts of Dr. Jian Liu (University of North Carolina) [39]. Recombinant keratanase II from *Bacillus circulans* was expressed and purified in our laboratory following our previous method [40]. 2-Aminoacridone (AMAC) and sodium cyanoborohydride ($NaCNBH_3$) were obtained from Sigma-Aldrich (St. Louis, MO). All other chemicals were of High Performance Liquid Chromatography (HPLC) grade. Vivapure Q Maxi and Mini H strong anion exchange spin columns were from Sartoriou Stedim Biotech (Bohemia, NY). Amicon Ultra-0.5 mL and 15 mL 3 K molecular-weight-cut-off (MWCO) Centrifugal Filters were purchased from MilliporeSigma (Burlington, MA).

Isolation of retina from porcine and axolotl eyes

The retina was isolated from porcine eyes collected fresh from the abattoir (Research 87 Inc., Boston) within 1 h after slaughter. Briefly, the muscle surrounding the eye was removed and the eyeball was hemisected with fine scissors to remove the cornea and the vitreous humour. The hemisected eyecup was flooded with phosphate buffer saline (phosphate buffered saline (PBS), Sigma–Aldrich) and the retina was peeled gently from the retinal pigment epithelium using a microspatula. The isolated retina was transferred into deionized (DI) water using a transfer pipette and shaken on an orbital shaker (TECHNE Mini Orbital Shaker, TSSM1) at 75 rpm for 3 min at room temperature. The retinas were collected using a transfer pipet and processed further for decellularization.

Axolotl eyes were enucleated immediately after the animal was sacrificed and placed in 1X PBS (~1 mL) in a 1.5 mL Eppendorf tube. Using straight forceps (Roboz surgical instruments), axolotl eye(s) were transferred to the lid of a 35 mm dish (Corning) filled with ~3 mL PBS. Briefly, connective tissue and muscle was removed from the back of the eye using angled and straight forceps with the aid of a dissecting microscope. With the cornea facing up, angled forceps were used to pinch up a small fold in the center of the cornea. Using spring scissors, a small incision was made at the base of the fold such that the eye was approximately cut in half, with both the cornea and iris removed in the top half. The remaining posterior half of the eye was pressed down gently, forcing the lens and vitreous humor out to be discarded. The inside of the remaining eyecup was lined by the retina, which lifts off as it delaminates from RPE. The isolated retina was collected using a transfer pipet and processed further for decellularization.

Decellularization of porcine and axolotl retina

Retinas isolated from porcine and axolotl eyes were decellularized with 1% sodium dodecyl sulfate (SDS). In brief, isolated porcine and axolotl retinas were transferred into tubes (15 mL falcon tubes for porcine retina/1.5 mL Eppendorf tubes for axolotl retina) containing 5 mL and 0.5 mL of 1% SDS solution, respectively, at room temperature. The tubes were then placed on the orbital shaker at 30 rpm for 1 h. The retinas were then harvested using a transfer pipet, minimizing the amount of transferred SDS, transferred into DI water and centrifuged at 25 °C at 10,000 rpm for 15 min. The supernatant was removed, and retinas were resuspended in DI water and harvested again using transfer pipette. The residual/bound SDS was removed by loading the retina suspension within dialysis tubing (MWCO 12,500, Sigma Aldrich) and dialyzing against DI water with several changes (8–10 times over a span of 48 h) to obtain the decellularized retina suspension.

Lyophilization of porcine and axolotl retina

Decellularized-retina/native retina suspension as obtained above was frozen in 1.5 mL Eppendorf tubes in −80 °C freezer (Thermo Electron) overnight and then subjected to lyophilization using a freeze drier (Flexi-Dry MP, Kinetics thermal systems) with the temperature maintained within the sample chamber (−55 to −85 °C) [41]. The decellularized retina samples were dried for 48 h to obtain lyophilized decellularized retina.

Hyaluronic acid (HA) staining of retina

The isolated pig retina and whole axolotl eye were fixed in 4% paraformaldehyde overnight at 4 °C. The samples were then washed with PBS, cryoprotected in 30% sucrose solution, mounted in Optimal Cutting Temperature embedding medium (Fisher HealthCare, Houston, TX), and cryosectioned at 15 μm thickness. The slides with sections were washed with filtered diH_2O, washed with PBS for 5 min, blocked in goat serum for 30 min (15:1000 in PBS), washed with PBS for 5 min, and incubated in the anti-hyaluronic acid primary antibody overnight at 4 °C (sheep polyclonal, 1:1000 in goat serum block, Abcam). The slides were then washed with PBS for 5 min, incubated in the secondary antibody for 30 min, (1:400 in PBS, Alexa Fluor™ 594 donkey anti-sheep IgG, Invitrogen), washed in PBS for 5 min, incubated with DAPI for 5 min, washed with PBS for 5 min, washed with filtered diH_2O for 5 min, and mounted with 80% glycerol. Control slides were incubated in goat serum overnight without the addition of a primary antibody.

Isolation of GAGs from porcine and axolotl retina tissues

Tissues were homogenized with acetone at room temperature for 1 h. Once acetone was completely removed, tissue was digested using Actinase E for 12–24 h. Completely digested tissues were lyophilized. Dry tissues were dissolved in 8 M urea and 2 wt% CHAPS (3-((3-cholamidopropyl) dimethylammonio)-1-propanesulfonate) buffer, and GAGs were purified using MAXI H spin columns. Permeate was collected and desalted using 3 kDa molecular weight cut-off spin columns and the retentate was collected and lyophilized (lyophilized GAG samples).

Digestion of GAG into CS (chondroitin sulfate), HS (heparan sulfate), and KS (keratan sulfate) disaccharides

Lyophilized GAG samples were treated with a mixture of recombinant heparinase I, II, and III, chondroitinase ABC, and keratanase in digestion buffer (20 mU each per every 1 mg of GAG in 50 mM ammonium acetate containing 2 mM calcium chloride adjusted to pH 7.0) at 37 °C for 5 h to prepare CS, HS, and KS disaccharides. The reaction was terminated by placing in a 100 °C water bath for 5 min. The reaction mixture was cooled and spun down in 3 kDa columns to collect disaccharide products.

AMAC labeling

The dried samples were AMAC (2-aminoacridone)-labeled by adding 10 μL of 0.1 M AMAC in DMSO/acetic acid (17/3, *v/v*) incubating at room temperature for 10 min, followed by adding 10 μL of 1 M aqueous $NaBH_3CN$ and incubating for 1 h at 45 °C. A mixture containing all 19-disaccharide standards prepared at 6.25 ng/μL was similarly AMAC-labeled and used for each run as an external standard. After the AMAC-labeling reaction, the samples were centrifuged and each supernatant was recovered.

Disaccharide analysis using liquid chromatography mass spectrometry (LC-MS)

LC-MS analyses were performed on an Agilent 1200 LC/MSD Instrument (Agilent Technologies, Inc., Wilmington, DE) equipped with a 6300 ion-trap and a binary pump. LC parameters: column: Agilent Poroshell 120 C18 column (2.7 μm 3.0 × 150 mm). The column temperature was 45 °C. The flow rate was 150 μL/min. The mobile phase was: A: 50 mM NH_4OAc in water; B: methanol; gradient: 0–20 min, 5–30% B; 20–30 min, 30–50% B; 30–40 min, 100% B; 40–50 min, 5% B. The MS parameters were electrospray in the negative ionization mode with a skimmer potential of −40.0 V, a capillary exit of −40.0 V, and a source temperature of 350 °C. The mass range of the spectrum was 300–900 m/z. Nitrogen (8 L/min 40 psi) was used as drying and nebulizing gas.

Results

Anatomy of axolotl and porcine retina

Retina is composed of six different neural cell types: cone and rod photoreceptors, horizontal, bipolar, amacrine and ganglion cells. The photoreceptor cells are localized in the posterior retina where they capture light and transform it into electrical signals [42]. The retinal layers are classified into the GCL (ganglion cell layer), the INL (inner nuclear layer), where the nuclei of amacrine, bipolar and horizontal cells are located, and the ONL (outer nuclear layer), which contains the nuclei of the photoreceptors [43]. The OPL (outer plexiform layer) is the location of synaptic connections between the photoreceptors with horizontal and/or bipolar cells. The IPL (inner plexiform layer) is the region where synaptic communication occurs between bipolar and ganglion cells [43]. All of these layers are present in both porcine and axolotl retina (Fig. 1). The region of the photoreceptor outer segments is larger in the axolotl retina than in the porcine retina. The size of the cell nuclei in the INL and ONL regions of the axolotl retina is bigger than those of the porcine cell nuclei, possibly due to the larger genome size of axolotl [36].

CS is the major GAG component in both axolotl and porcine retina

Native retina and decellularized retina tissues were collected from six individual pigs and four individual axolotls. GAGs were recovered from tissues from each individual animal tissue sample, treated with polysaccharide lyases and subjected to high performance liquid chromatography-mass spectrometry (HPLC-MS) to obtain their GAG disaccharide composition. The major GAG in native axolotl, native porcine, decellularized axolotl, and decellularized porcine retina, was CS corresponding to 31.8%, 44.4%, 31.3%, and 35.9% (44.9 ng/mg, 34.8 ng/mg, 13.5 ng/mg, and 12.9 ng/mg), respectively, of the total GAG content (Fig. 2). The second most prominent GAG was either HS or HA, depending on the tissue sample analyzed. In native axolotl, native porcine, decellularized axolotl, and decellularized porcine retina the total HS was 13.9%, 33.8.6%, 22.0%, and 52.7% (22.7 ng/mg, 25.7 ng/mg, 8.7 ng/mg, and 18.8 ng/mg), and the total HA was 52.3%, 12.9%, 39.1%, and 4.9% (77.6 ng/mg, 10.5 ng/mg, 16.9 ng/mg, and 1.8 ng/mg), respectively. The KS content of all of the retinal samples was quite low, ranging from 1.9 to 8.8% (2.3 to 6.9 ng/mg).

Higher levels of sulfated disaccharides, 4S, 6S, and lower levels of unsulfated disaccharide, 0S, in axolotl retinal CS

Next, the CS composition of axolotl and porcine samples were examined. The triS, 2S6S, 2S4S, 4S6S, and 2S disaccharides were absent from all retina tissue samples. In both native and decellularized retina, axolotl CS was comprised of significantly more 4S and 6S disaccharides, but of less 0S disaccharides than porcine retinal CS. Native axolotl retinal CS was comprised of 4S, 6S, and 0S disaccharides at 17.2%, 11.0%, and 3.6%, respectively. In contrast, native porcine retinal CS was comprised of 4S and 0S, 5.6% and 38.8%, respectively, however it contained no detectable 6S disaccharide. In decellularized axolotl retinal CS, the 4S, 6S, and 0S composition was 18.5%, 7.8%, and 4.9%, respectively. In the decellularized porcine retinal CS the 4S and 0S disaccharide composition was 15.5% and 20.4% were present. KS mono-S disaccharide was present in all four tissues.

Greater levels of HA in axolotl retina was indicated using both LCMS and immunohistochemical methods

More HA was observed in axolotl retina compared to porcine retina in both native and decellularized tissues (Figs. 2 and 4). Native axolotl retina had a higher HA composition, 52.3%, compared to that of native porcine retina at 12.9%. Similarly, HA composition in decellularized axolotl, 39.1%, was greater than that in decellularized porcine retina, at 4.9%. We also performed immunohistochemical staining of HA in native axolotl and porcine retina to qualitatively validate this finding (Fig. 1) and the results obtained agree with HPLC-MS GAG analysis. In the axolotl retina, expression of HA was perinuclear, suggesting its localization in the ECM. HA was detected throughout the axolotl retina, with a particularly strong expression in GCL and RPE. In contrast, the expression of HA was lower in the porcine retina and it was not observed in ONL, INL, or GCL.

Lower levels of unsulfated 0S disaccharide in axolotl retinal HS

Several trends were observed in the composition of axolotl and porcine retinal HS (Figs. 2 and 4). In terms of the percentage of total GAG that was HS, axolotl retina was considerably lower than porcine retina in both native and decellularized samples (Fig. 2). The composition of HS in native and decellularized axolotl retina showed 0S disaccharide levels of 3.4% and 10.2%, respectively, considerably lower than the 0S disaccharide levels ofnative and decellularized porcine retina of 31.8% and 20.5%, respectively. The NS2S, NS, 6S, and 2S disaccharides were present in native axolotl HS as minor components at 1.6, 5.1, 3.7, and 0.2%, respectively, however, only the 6S was detected (at 2.1%) in the HS of the native porcine retina. The 6S is present in the HS of decellularized axolotl retina at 2.1%. The NS, 6S and 2S are also present in the HS of decellularized porcine retina at 8.0, 2.6, and 1.3%, respectively. The highly sulfated TriS, NS6S, and 2S6S disaccharides were absent in all of the retinal tissue samples.

Discussion

In this study, we performed systematic GAG compositional analysis ofnative and decellularized axolotl and porcine retina to investigate how the distribution of GAGs from axolotl retina and its ECM environment differentiate from those of porcine retina during homeostatic conditions in an attempt to find clues to the retinal regenerative capacity of urodele axolotl throughout its lifespan. Porcine retina served as a mammalian vertebrate model lacking regenerative ability during adulthood that is similar to the regenerative inability of human retina. From these analyses, we learned that the major retinal GAG is CS (31.3–44.4% or 12.9–44.9 ng/mg) followed by HS (13.9–52.7% or 8.7–25.7 ng/mg) and HA (4.9–52.3% or 1.8–77.6 ng/mg) and KS (1.9–8.8% or 2.3–6.9 ng/mg) collected from both native and decellularized axolotl and porcine retina (Fig. 2). The observation that CS was the dominant GAG in the retina is consistent with previous literature on bovine retinal pericyte culture and for the human retina [31, 44]. CS is distributed mainly in two regions, nerve fibers and the interphotoreceptor matrix (IPM) including the surface of RPE cells [31]. Among some of the known proteoglycans carrying the CS GAG chain in the retina are neurocan and phosphacan, which are exclusive to nervous tissue and are upregulated during retinal development but downregulated at retinal maturation. In a healthy human eye, CS 0S is observed throughout the retina along with CS 6S as another major CS disaccharide in IPM [44]. In the rat retina, CS 6S was also present in IPM, however, CS 4S is reportedly absent [45]. Our findings are in accordance with previous studies except for some notable differences between axolotl and porcine retina (Fig. 3). In both native and decellularized retina, the axolotl retina has significantly greater levels ofCS 6S and CS 4S to a less extent than those of porcine retina. Significantly lower level of CS 0S was also found in native and decellularized axolotl retina compared to that of porcine retina. The inhibitory roles of CS in retinal axonal outgrowth and integration of stem cell transplant in retinal degeneration model have been reported [29, 46–48]; however, positive effect of CS also has been associated with neuronal patterning in the retina and neuroprotective activity of retinal cells in intraocular pressure defect models [49, 50]. Lower level of CS 0S and greater levels of CS 4S and 6S in native and decellularized retina collected from axolotl in homeostatic conditions, compared

to those of porcine retina, are novel findings and may be further investigated during retinal injury and regeneration.

Next, both native and decellularized axolotl retina exhibited greater level of HA compared to those of porcine, validated by both LCMS and immunohistochemical analytical methods (Figs. 1, 2, and 4). HA-specific staining of retina collected from fetal and adult (ranging from 28 to 94 years of age) human donors showed that HA expression decreased with age in the choroid, RPE, and Bruch's membrane [51]. HA is a prominent component of the IPM in human, bovine, guinea pig, dog, and rat with the exception of mouse [52]. In the embryonic chick retina, HA synthase expression was increased until the postnatal day 1, however was reduced in adulthood [53]. HA was also found to inhibit CS synthesis and accumulation of newly synthesized PGs in the chick embryo chondrocytes *in vitro* [54]. This is an interesting finding, because it suggests HA may have protective effects against the known inhibitory role of CS in CNS regeneration. HA synthesis is required in limb and lens regeneration of amphibians, chick embryo limb generation through induction of basic FGF, and tail fin regeneration in zebrafish [23, 34, 35, 55]. In another urodele species *Triturus alpestris*, total GAG amounts were reported to be approximately 50 to 140 μg/mg dry tissue during regeneration of limbs and tail [23]. In addition, HA is FDA-approved to treat retinal detachment in human [56]. In the case of urodele newts, significant accumulation of HA (~2300 dpm/mg dry tissue) was observed in the dorsal iris compared to the controls (up to 450 dpm/mg dry tissue) during the course of lens regeneration. (accumulation of HA was determined by examining the level of [^{3}H]glucosamine label incorporated into HA) [25]. Increased levels of HA in the axolotl retina suggest promising potential role of GAG in its pro-regenerative environment.

Lastly, both native and decellularized axolotl retina exhibited a lower level of HS 0S disaccharide, and other sulfated HS disaccharides were mainly found in decellularized retina of both axolotl and pig. Soluble HSPGs are found in the extracellular matrices of the basement membrane, while HS anchored to the core proteins are localized mainly in the neurites of retinal neuronal cells, implicating their function in cytokine signaling [31]. Our disaccharide analysis shows that HS composition is greater in decellularized tissues, resembling the ECM space, in both axolotl and porcine retina by 22.0% and 52.7%, respectively. Soluble HS has been associated with induction of neurite outgrowth through FGF signaling in rat retinal ganglion cells in ECM, and retinal regeneration in amphibian is inhibited when the laminin-HSPG interaction is disrupted [57, 58]. Membrane-bound HSPGs have been implicated in retinal neuronal cell adhesion and retinal neurite outgrowth through FGF signaling [59–61]. FGF signaling is regulated by the sulfation pattern and chain length of HS [62], thus, the differential sulfation patterns of decellularized axolotl retinal HS compared to that of pig may be critical for FGF-binding and ultimately retinal regenerative capacity of axolotl. While present in smaller amounts relative to other GAGs, HS disaccharides and their composition in the native axolotl retina may be relevant to retinal regenerative ability. In the native axolotl retina, higher levels of HS NS2S and HS NS and lower levels HS 0S were observed, which is in better agreement with the HS disaccharide composition pattern of young (average 32 years old) human retina than for old (average 82 years old) human retina in the Bruch's membrane [63]. In the context of AMD, this differential HS composition was associated with binding to complement factor H (CFH). In

the axolotl, limb regeneration is also mediated by HS allowing position-specific memory in ECM through FGF signaling [27].

While we were able to discover distinctive GAG profile of the axolotl retina in comparison with porcine retinal GAG profile during homeostatic conditions for the first time, more studies can further our insight into the role of GAGs in the axolotl retina. For example, GAG composition analysis and immunohistochemical staining can be performed in GAG isolated from axolotl retina collected during various time points after retinal injury and in regions undergoing neurogenesis to detect change in relative amount and composition of GAGs and the sulfation patterns. Transcriptomic analysis of enzymes involved in GAG synthesis and GAG binding proteins may further facilitate our understanding of not only the expression of GAGs, but also partners interacting with GAGs during retinal injury and regeneration. Together, these findings may assist our fundamental understanding of retinal degeneration and regeneration and designing therapeutic approaches for vision loss from a carbohydrate perspective.

Acknowledgements

This research was funded by the NIH in the form of grants DK111958, CA231074, HL125371 (to RJL) and by grant NSF-CBET #1606128 (to RLC).

References

1. Wong WL, Su X, Li X, Cheung CM, Klein R, Cheng CY, Wong TY: Global prevalence of age-related macular degeneration and disease burden projection for 2020 and 2040: a systematic review and meta-analysis. Lancet Glob. Health. 2, e106–e116 (2014) [PubMed: 25104651]
2. Barbosa-Sabanero K, Hoffmann A, Judge C, Lightcap N, Tsonis PA, Del Rio-Tsonis K: Lens and retina regeneration: new perspectives from model organisms. Biochem. J. 447, 321334 (2012)
3. Del Rio-Tsonis K, Tsonis PA: Eye regeneration at the molecular age. Dev. Dyn. 226, 211–224 (2003) [PubMed: 12557200]
4. Haynes T, Del Rio-Tsonis K: Retina repair, stem cells and beyond. Curr. Neurovasc. Res. 1, 231–239 (2004) [PubMed: 16181073]
5. Hayashi T, Mizuno N, Ueda Y, Okamoto M, Kondoh H: FGF2 triggers iris-derived lens regeneration in newt eye. Mech. Dev. 121, 519–526 (2004) [PubMed: 15172683]
6. Spence JR, Aycinena JC, Del Rio-Tsonis K: Fibroblast growth factor-hedgehog interdependence during retina regeneration. Dev. Dyn. 236, 1161–1174 (2007) [PubMed: 17385725]
7. Susaki K, Chiba C: MEK mediates *in vitro* neural transdifferentiation of the adult newt retinal pigment epithelium cells: is FGF2 an induction factor? Pigment Cell Res. 20, 364379 (2007)
8. Spence JR, Madhavan M, Aycinena JC, Del Rio-Tsonis K: Retina regeneration in the chick embryo is not induced by spontaneous Mitf downregulation but requires FGF/FGFR/MEK/Erk dependent upregulation ofPax6. Mol. Vis. 13, 57–65 (2007) [PubMed: 17277739]
9. Schlessinger J, Plotnikov AN, Ibrahimi OA, Eliseenkova AV, Yeh BK, Yayon A, Linhardt RJ, Mohammadi M: Crystal structure of a ternary FGF-FGFR-heparin complex reveals a dual role for heparin in FGFR binding and dimerization. Mol. Cell. 6, 743–750 (2000) [PubMed: 11030354]
10. Sterner E, Meli L, Kwon SJ, Dordick JS, Linhardt RJ: FGF-FGFR signaling mediated through glycosaminoglycans in microtiter plate and cell-based microarray platforms. Biochemistry. 50, 9009–9019 (2013)
11. Linhardt RJ, Toida T: Role of glycosaminoglycans in cellular communication. Acc. Chem. Res. 7, 431–438 (2004)

12. Kim SY, Zhao J, Liu X, Fraser K, Lin L, Zhang X, Zhang F, Dordick JS, Linhardt RJ: Interaction of Zika virus envelope protein with glycosaminoglycans. Biochemistry. 56, 1151–1162 (2017) [PubMed: 28151637]
13. Kim SY, Zhang F, Gong W, Chen K, Xia K, Liu F, Gross RA, Wang JM, Linhardt RJ, Cotton ML: Copper regulates the interactions of antimicrobial piscidin peptides from fish mast cells with formyl peptide receptors and heparin. J. Biol. Chem. 293, 15381–15396 (2018) [PubMed: 30158246]
14. Kaprinis K, Symeonidis C, Papakonstantinou E, Tsinopoulos I, Dimitrakos SA: Decreased hyaluronan concentration during primary rhegmatogenous retinal detachment. Eur. J. Ophthalmol. 26, 633–638 (2016) [PubMed: 27198637]
15. Park PJ., Shukla D: Role of heparan sulfate in ocular diseases. Exp. Eye Res. 110, 1–9 (2013) [PubMed: 23410824]
16. McManus LM, Mitchell RN: Pathobiology of human disease: a dynamic encyclopedia of disease mechanisms. Elsevier (2014)
17. Dreyfuss JL, Regatieri CV, Lima MA, Paredes-Gamero EJ, Brito AS, Chavante SF, Belfort R Jr., Farah ME, Nader HB: A heparin mimetic isolated from a marine shrimp suppresses neovascularization. J. Thromb. Haemost. 8, 1828–1837 (2010) [PubMed: 20492474]
18. Jiang X, Couchman JR: Perlecan and tumor angiogenesis. J. Histochem. Cytochem. 51, 1393–1410 (2003) [PubMed: 14566013]
19. Regatieri CV, Dreyfuss JL, Melo GB, Lavinsky D, Hossaka SK, Rodrigues EB, Farah ME, Maia M, Nader HB: Quantitative evaluation of experimental choroidal neovascularization by confocal scanning laser ophthalmoscopy: fluorescein angiogram parallels heparan sulfate proteoglycan expression. Braz. J. Med. Biol. Res. 43, 627–633 (2010) [PubMed: 20464343]
20. Clark SJ, Bishop PN, Day AJ: Complement factor H and age-related macular degeneration: the role of glycosaminoglycan recognition in disease pathology. Biochem. Soc. Trans. 38, 1342–1348 (2010) [PubMed: 20863311]
21. Clark SJ, Perveen R, Hakobyan S, Morgan BP, Sim RB, Bishop PN, Day AJ: Impaired binding of the age-related macular degeneration-associated complement factor H 402H allotype to Bruch's membrane in human retina. J. Biol. Chem. 285, 192–202 (2010)
22. Kelly U, Yu L, Kumar P, Ding JD, Jiang H, Hageman GS, Arshavsky VY, Frank MM, Hauser MA, Rickman CB: Heparan sulfate, including that in Bruch's membrane, inhibits the complement alternative pathway: implications for age-related macular degeneration. J. Immunol. 185, 5486–5494 (2010) [PubMed: 20876352]
23. Alibardi L: Hyaluronic acid in the tail and limb of amphibians and lizards recreates permissive embryonic conditions for regeneration due to its hygroscopic and immunosuppressive properties. J Exp Zool B Mol Dev Evol. 328, 760–771 (2017) [PubMed: 29106045]
24. Ouyang X, Panetta NJ, Talbott MD, Payumo AY, Halluin C, Longaker MT, Chen JK: Hyaluronic acid synthesis is required for zebrafish tail fin regeneration. PLoS One. 12, e0171898 (2017) [PubMed: 28207787]
25. Kulyk WM, Zalik SE, Dimitrov E: Hyaluronic acid production and hyaluronidase activity in the newt iris during lens regeneration. Exp. Cell Res. 172, 180–191 (1987) [PubMed: 3653253]
26. Gardiner DM: Regulation of regeneration by heparan sulfate proteoglycans in the extracellular matrix. Regen Eng Transl Med. 3, 192–198 (2017) [PubMed: 29242821]
27. Phan AQ, Lee J, Oei M, Flath C, Hwe C, Mariano R, Vu T, Shu C, Dinh A, Simkin J, Muneoka K, Bryant SV, Gardiner DM: Positional information in axolotl and mouse limb extracellular matrix is mediated via heparan sulfate and fibroblast growth factor during limb regeneration in the axolotl (Ambystoma mexicanum). Regeneration. 2, 182–201 (2015) [PubMed: 27499874]
28. Ramachandra R, Namburi RB, Dupont ST, Ortega-Martinez O, van Kuppevelt TH, Lindahl U, Spillmann D: A potential role for chondroitin sulfate/dermatan sulfate in arm regeneration in Amphiura filiformis. Glycobiology. 27, 438–449 (2017) [PubMed: 28130266]
29. Becker CG, Becker T: Repellent guidance of regenerating optic axons by chondroitin sulfate glycosaminoglycans in zebrafish. J. Neurosci. 22, 842–853 (2002) [PubMed: 11826114]

30. Rauvala H, Paveliev M, Kuja-Panula J, Kulesskaya N: Inhibition and enhancement of neural regeneration by chondroitin sulfate proteoglycans. Neural Regen. Res. 12, 687–691 (2017) [PubMed: 28616017]
31. Inatani M, Tanihara H: Proteoglycans in retina. Prog. Retin. Eye Res. 21, 429–447 (2002) [PubMed: 12207944]
32. Joven A, Simon A: Homeostatic and regenerative neurogenesis in salamanders. Prog. Neurobiol. 170, 81–98 (2018) [PubMed: 29654836]
33. Roy S, Levesque M: Limb regeneration in axolotl: is it superhealing? Sci. World J. 6, 12–25 (2006)
34. Alunni A, Bally-Cuif L: A comparative view of regenerative neurogenesis invertebrates. Development. 143, 741–753 (2016) [PubMed: 26932669]
35. Sun YB, Xiong ZJ, Xiang XY, Liu SP, Zhou WW, Tu XL, Zhong L, Wang L, Wu DD, Zhang BL, Zhu CL: Whole-genome sequence of the Tibetan frog Nanorana parkeri and the comparative evolution of tetrapod genomes. Proc. Natl. Acad. Sci. 112, 1257–1262 (2015)
36. Nowoshilow S, Schloissnig S, Fei JF, Dahl A, Pang AW, Pippel M, Winkler S, Hastie AR, Young G, Roscito JG, Falcon F: The axolotl genome and the evolution of key tissue formation regulators. Nature. 554, 50–55 (2018) [PubMed: 29364872]
37. Svistunov SA, Mitashov VI: Proliferative activity ofthe pigment epithelium and regenerating retinal cells in Ambystoma mexicanum. Ontogenez. 14, 597–606 (1983) [PubMed: 6657169]
38. Voss SR, Epperlein HH, Tanaka EM: *Ambystoma mexicanum*, the axolotl: a versatile amphibian model for regeneration, development, and evolution studies. Cold Spring Harb Protoc. 8, pdb.emo128, (2009)
39. Linhardt RJ, Turnbull JE, Wang HM, Loganathan D, Gallagher JT: Examination ofthe substrate specificity of heparin and heparan sulfate lyases. Biochemistry. 29, 2611–2617 (1990) [PubMed: 2334685]
40. Wang H, He W, Jiang P, Yu Y, Lin L, Sun X, Koffas M, Zhang F, Linhardt RJ: Construction and functional characterization of truncated versions of recombinant keratanase II from Bacillus circulans. Glycoconj. J. 34, 643–649 (2017) [PubMed: 28752383]
41. Kundu J, Michaelson A, Talbot K, Baranov P, Young MJ, Carrier RL: Decellularized retinal matrix: natural platforms for human retinal progenitor cell culture. Acta Biomater. 31, 61–70 (2016) [PubMed: 26621699]
42. Wright AF, Chakarova CF, El-Aziz MM, Bhattacharya SS: Photoreceptor degeneration: genetic and mechanistic dissection of a complex trait. Nat Rev Genet. 11, 273–284 (2010) [PubMed: 20212494]
43. Grzybowski A: General structure and function of the retina. Acta Ophthalmol. 94, (2016)
44. Sanchez I, Martin R, Ussa F, Fernandez-Bueno I: The parameters of the porcine eyeball. Graefes Arch. Clin. Exp. Ophthalmol. 249, 475–482 (2011) [PubMed: 21287191]
45. Porrello K, Lavail MM: Immunocytochemical localization of chondroitin sulfates in the interphotoreceptor matrix of the normal and dystrophic rat retina. Curr. Eye Res. 5, 981–993 (1986) [PubMed: 3100143]
46. Singhal S, Lawrence JM, Bhatia B, Ellis JS, Kwan AS, MacNeil A, Luthert PJ., Fawcett JW, Perez MT, Khaw PT, Limb GA: Chondroitin sulfate proteoglycans and microglia prevent migration and integration of grafted Muller stem cells into degenerating retina. Stem Cells. 26, 1074–1082 (2008) [PubMed: 18218817]
47. Suzuki T, Akimoto M, Imai H, Ueda Y, Mandai M, Yoshimura N, Swaroop A, Takahashi M: Chondroitinase ABC treatment enhances synaptogenesis between transplant and host neurons in model of retinal degeneration. Cell Transplant. 16, 493–503 (2007) [PubMed: 17708339]
48. Ichijo H, Kawabata I: Roles of the telencephalic cells and their chondroitin sulfate proteoglycans in delimiting an anterior border of the retinal pathway. J. Neurosci. 21, 9304–9314 (2001) [PubMed: 11717364]
49. Brittis PA, Canning DR, Silver J: Chondroitin sulfate as a regulator of neuronal patterning in the retina. Science. 255, 733736 (1992)
50. Bakalash S, Rolls A, Lider O, Schwartz M: Chondroitin sulfate-derived disaccharide protects retinal cells from elevated intraocular pressure in aged and immunocompromised rats. Invest. Ophthalmol. Vis. Sci. 48, 1181–1190 (2007) [PubMed: 17325162]

51. Tate DJ, Oliver PD, Miceli MV, Stern R, Shuster S, Newsome DA: Age-dependent change in the hyaluronic acid content of the human chorioretinal complex. Arch. Ophthalmol. 111, 963–967 (1993) [PubMed: 8328939]
52. Hollyfield JG, Rayborn ME, Tammi M, Tammi R: Hyaluronan in the interphotoreceptor matrix of the eye: species differences in content, distribution, ligand binding and degradation. Exp. Eye Res. 66, 241–248 (1998) [PubMed: 9533850]
53. Inoue Y, Yoneda M, Miyaishi O, Iwaki M, Zako M: Hyaluronan dynamics during retinal development. Brain Res. 1256, 55–60 (2009) [PubMed: 19124007]
54. Solursh M, Vaerewyck SA, Reiter RS: Depression by hyaluronic acid of glycosaminoglycan synthesis by cultured chick embryo chondrocytes. Dev. Biol. 41, 233–244 (1974) [PubMed: 4281397]
55. Munaim SI, Klagsbrun M, Toole BP: Hyaluronan-dependent pericellular coats of chick embryo limb mesodermal cells: induction by basic fibroblast growth factor. Dev. Biol. 143, 297–302 (1991) [PubMed: 1899405]
56. Vatne HO, Syrdalen P: The use of sodium hyaluronate (Healon) in the treatment of complicated cases of retinal detachment. Acta Ophthalmol. 64(169–172), (1986)
57. Lipton SA, Wagner JA, Madison RD, D'Amore PA: Acidic fibroblast growth factor enhances regeneration of processes by postnatal mammalian retinal ganglion cells in culture. Proc. Natl. Acad. Sci. U. S. A. 85, 2388–2392 (1988) [PubMed: 3353388]
58. Nagy T, Reh TA: Inhibition of retinal regeneration in larval Rana by an antibody directed against a laminin-heparan sulfate proteoglycan. Brain Res. Dev. 81, 131–134 (1994)
59. Schubert D, LaCorbiere M: Isolation of a cell-surface receptor for chick neural retina adherons. J. Cell Biol. 100, 56–63 (1985) [PubMed: 3965479]
60. Carri NG, Perris R, Johansson S, Ebendal T: Differential outgrowth of retinal neurites on purified extracellular matrix molecules. J. Neurosci. Res. 19, 428–439 (1988) [PubMed: 2455066]
61. Chernousov MA, Carey DJ: N-syndecan (Syndecan 3) from neonatal rat brain binds basic fibroblast growth factor. J. Biol. Chem. 268, 16810–16814 (1993) [PubMed: 8344959]
62. Ornitz DM, Itoh N: The fibroblast growth factor signaling pathway. Wiley Interdiscip. Rev. Dev. Biol. 4, 215–266 (2015) [PubMed: 25772309]
63. Keenan TD, Pickford CE, Holley RJ, Clark SJ, Lin W, Dowsey AW, Merry CL, Day AJ, Bishop PN: Age-dependent changes in heparan sulfate in human Bruch's membrane: implications for age-related macular degeneration. Invest. Ophthalmol. Vis. Sci. 55, 5370–5379 (2014) [PubMed: 25074778]

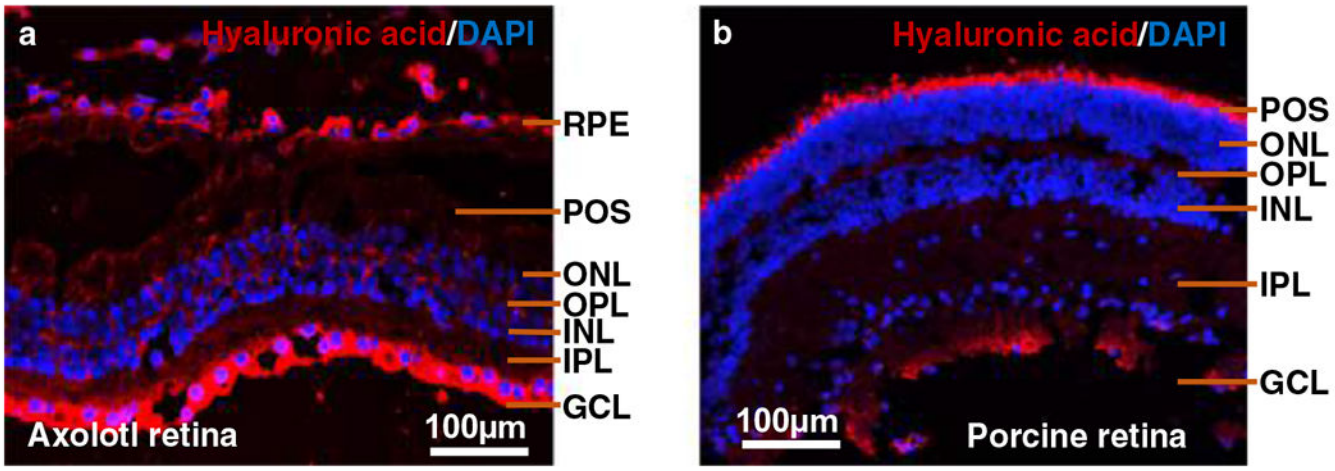

Fig. 1.

Cross-sectional anatomy of the (**a**) Axolotl and (**b**) porcine retina. Immunohistochemistry was performed to visualize expression of hyaluronic acid in the axolotl and porcine retina. Primary antibody (anti-hyaluronic acid sheep polyclonal, 1:1000 in goat serum block, Abcam) and secondary antibody (1:400 in PBS, Alexa FluorTM 594 donkey anti-sheep IgG, Invitrogen) were used to stain HA red while DAPI used to stain the nucleus blue. POS: Photoreceptor outer segments; ONL: outer nuclear layer; OPL: outer plexiform layer; INL: Inner nuclear layer; IPL: Inner plexiform layer; GCL: Ganglionic cell layer; RPE: Retinal pigment epithelium

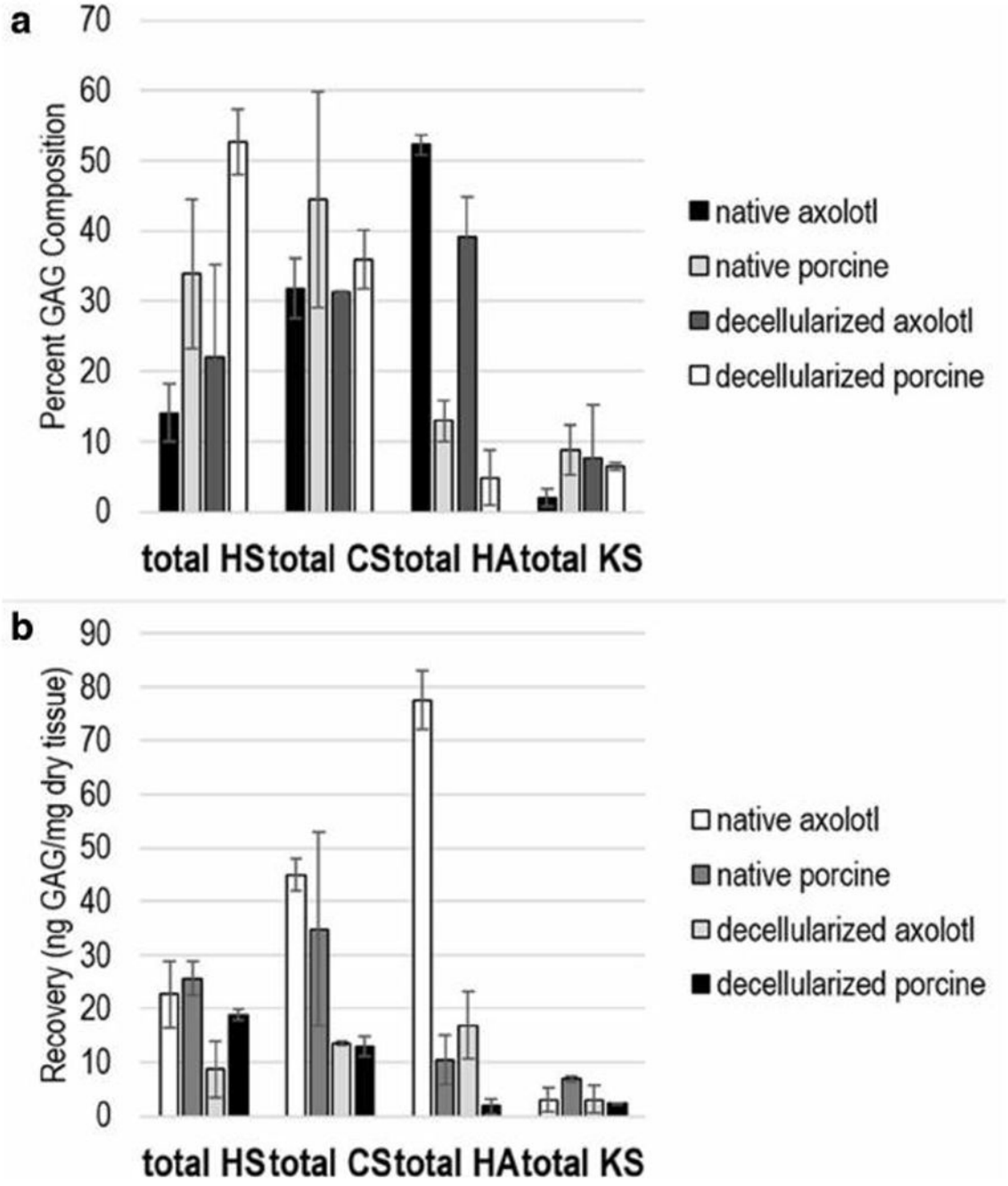

Fig. 2.

a GAG composition profile of total HS, CS, HA, and KS in native and decellularized axolotl and porcine retina. **b** amount of total HS, CS, HA, and KS in native and decellularized axolotl and porcine retina. The error bars represent standard deviation from the biological variability (four axolotl and six porcine for both native and decellularized). Each biological sample was run in triplicates (these error bars not shown)

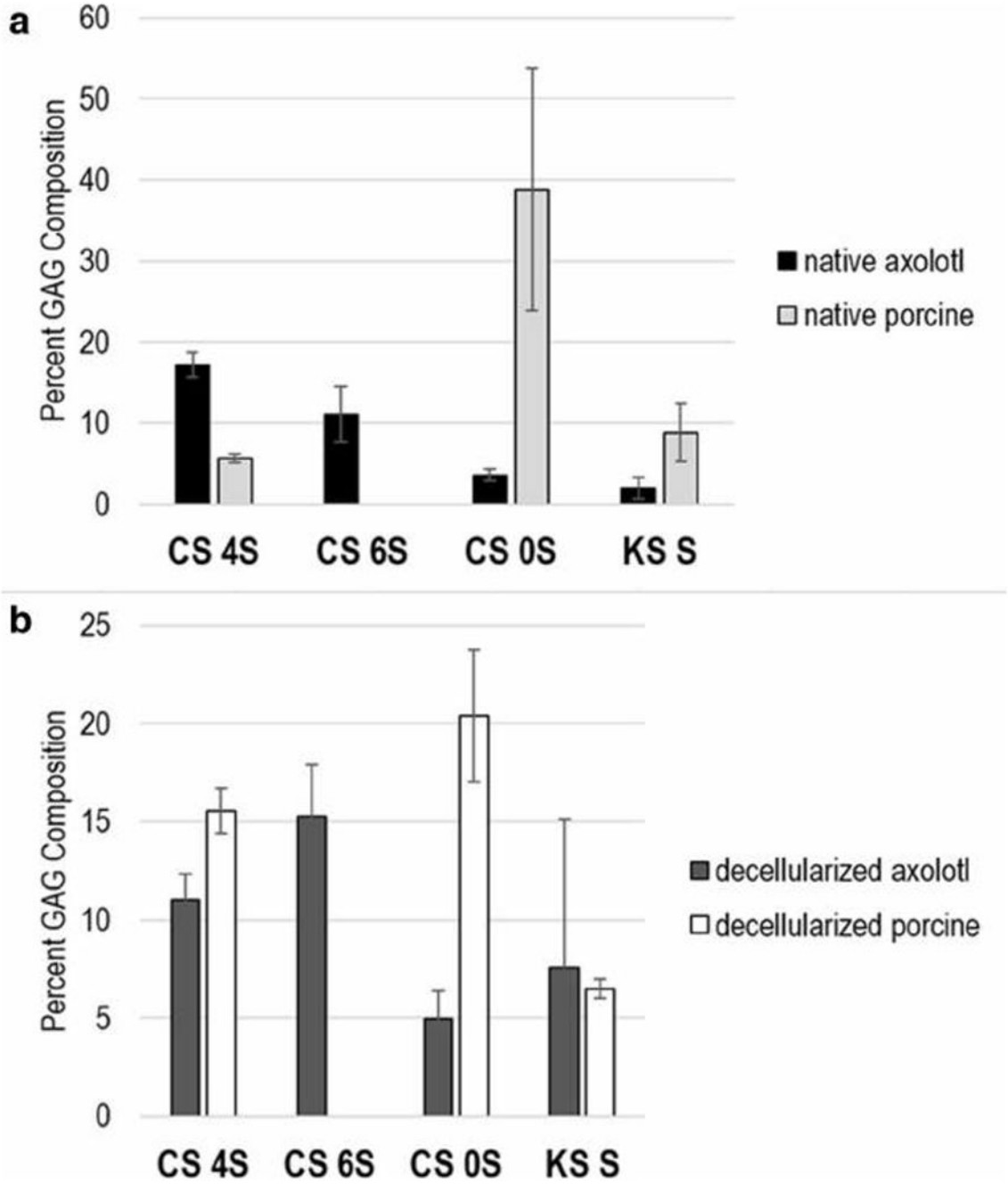

Fig. 3.

a GAG composition profile of CS and KS disaccharides from native axolotl and porcine retina. **b** GAG composition profile of CS and KS disaccharides from decellularized axolotl and porcine retina. The error bars represent standard deviation from the biological variability (four axolotl and six porcine for both native and decellularized). Each biological sample was run in triplicates (these error bars not shown)

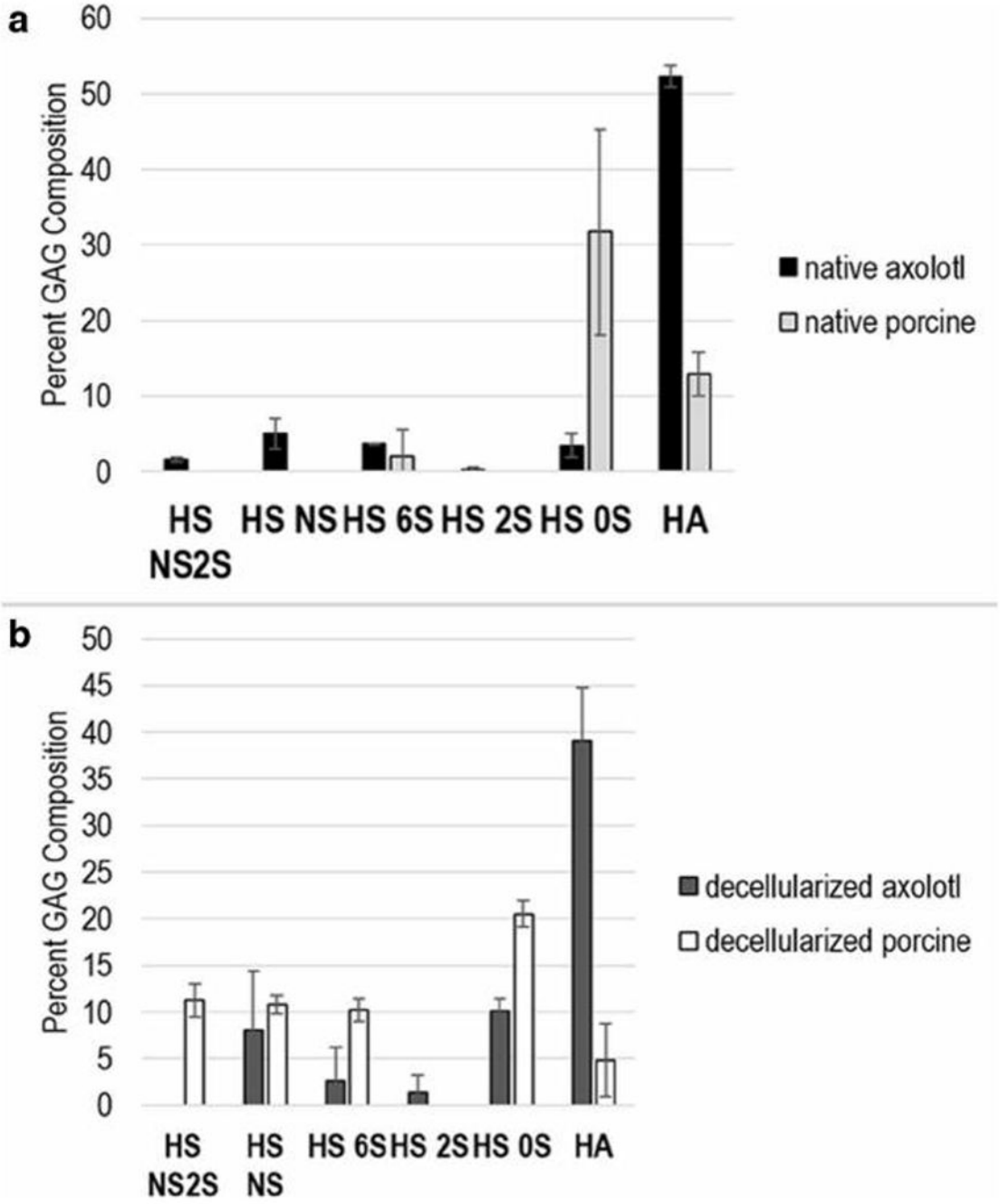

Fig. 4.

a GAG composition profile of HS and HA disaccharides from native axolotl and porcine retina. **b** GAG composition profile of total HS and HA disaccharides from decellularized axolotl and porcine retina. The error bars indicate standard deviation from the biological variability (four axolotl and six porcine for both native and decellularized). Each biological sample was run in triplicates (these error bars not shown)